Identification of two critical charge carrier doping values in high-temperature $Y_{0.8}Ca_{0.2}Ba_2Cu_3O_x$ and $Sm_{2-x}Ce_xCuO_{4-y}$ cuprate superconductors

B. J. Taylor, R. E. Baumbach, D. J. Scanderbeg, and M. B. Maple
Department of Physics, University of California–San Diego, La Jolla, California 92093, USA
(Received 15 April 2010; published 11 May 2010)

Despite over two decades of intense scrutiny, much controversy surrounds many of the most prominent characteristic phenomena found in the high-T_c cuprate-based superconductors. These include the pseudogap, the presence or absence of charge/spin ordering at 1/8 doping, the evolution of the Fermi surface with charge doping, and the physics determining the magnetic field-temperature phase boundary between the electrically dissipationless and dissipative mixed states, $H_g(T)$. From an analysis of the evolution of $H_g(T)$ of thin-film samples of $Y_{0.8}Ca_{0.2}Ba_2Cu_3O_x$ and $Sm_{2-x}Ce_xCuO_{4-y}$ with oxygen and Ce doping, respectively, we observe that the proximity to the doping state $p_{c1}=1/8$ and to the putative quantum-critical point of the pseudogap $p_{c2}\approx 0.195$ both have a quantifiable impact on the shape of $H_g(T)$.

DOI: 10.1103/PhysRevB.81.174511 PACS number(s): 74.72.Kf, 74.40.Kb

Of the many characteristic phenomena found in the high-T_c cuprate superconductors, two controversial issues, in particular, standout as among the most critical to developing a full understanding of these materials; the nature of the pseudogap phase, and the existence and/or importance of "stripe" phases arising from the 1/8 doping state; the doping region where evidence points to a likely reconstruction of the Fermi surface.[1] Hence they are also included in the most hotly debated issues with proponents arguing that the physics underlying each phenomenon holds the answer to the mechanism of superconductivity.[2–5] The issue remains open, for both the hole- and electron-doped cuprates, as to whether the pseudogap state competes with, or is a precursor to the superconducting state. Controversy remains as to whether or not the state extends into the superconducting phase encompassed by the "T_c-x dome,"[6–8] since results vary depending on the materials examined and on the types of measurements made.[2,9,10] Furthermore, there is disagreement as to whether or not the carrier concentration at which the pseudogap appears to terminate at $T=0$ is a quantum-critical point (QCP) and hence results in order-parameter fluctuations that provide the driving mechanism of superconductivity.[2,3] Similarly, phenomena such as charge/spin stripes have been associated with the 1/8 doping state,[11,12] and it is argued that stripe formation is a common characteristic in the cuprates and under certain conditions can mediate superconducting electron pairing in cuprates.[4,5] The existence of a QCP in the overdoped regime of high-T_c cuprates is challenged by the recent work of Cooper *et al.*[13] on the $La_{2-x}Sr_xCuO_4$ system. From measurements of low-temperature in-plane resistivity and a subsequent dual-component analysis, they find a T-linear contribution to the resistivity throughout the right-hand side of the superconducting dome that extends to doping concentrations beyond the superconducting region; hence, the pure Fermi-liquid state is never reached before superconductivity expires. It is suggested that this behavior is to be associated with an "extended quantum phase" rather than a QCP. Furthermore, they observe abrupt anticorrelated changes in the values of the coefficients of the T-linear and T^2 resistivity components, α_1 and α_2, respectively, with doping at the concentration $p_c\approx 0.19$, which is generally identified with the location of the QCP associated with the pseudogap phase. A scenario emerges where p_c is thought to coincide with the onset of incoherent normal-state transport at all finite temperatures for concentrations $p\leq p_c$, to which the pseudogap forms in response as an effort to lower the energy of the electronic ground state.

We address the relationship of all the above issues to that of the vortex solid to liquid boundary $H_g(T)$ of films of the hole-doped $Y_{0.8}Ca_{0.2}Ba_2Cu_3O_x$ and electron-doped $Sm_{2-x}Ce_xCuO_{4-y}$ systems in this study. Since the transport properties of the electronic states within the vortex core are anticipated to have an impact on the dynamical properties of vortices in the region of the vortex-solid-vortex-liquid phase transition,[14,15] measurements of the temperature field dependence of this boundary as a function of charge doping can serve to reveal the evolving nature of the underlying electronic species. The $H_g(T)$ line of the $Y_{0.8}Ca_{0.2}Ba_2Cu_3O_x$ films in this study was established from electrical transport measurements in magnetic fields up to 35 T with the applied field H $\|$ to the film c axis, as described below. Subsequently, the $H_g(T)$ data, shown in Fig. 1, were analyzed within the context of an empirically modified[14,15] form of the quantum-thermal vortex lattice melting model of Blatter and Ivlev[16] which was used to analyze similar data of both films and single crystals of high-T_c cuprates. The $H_g(T)$ data of the $Sm_{2-x}Ce_xCuO_{4-y}$ system has been previously reported[17] but not analyzed in the context of this model. We report here two key observations concerning the evolution of $H_g(T)$ with charge doping. For the $Y_{0.8}Ca_{0.2}Ba_2Cu_3O_x$ system, we observe: (1) the temperature field H-T dependence of $H_g(T)$ of samples with hole-doping levels above and below $p\approx 1/8$ are unambiguously distinct, with the former scaling simply with the value of the critical temperature T_c and the $T=0$ value of the upper critical field $H_{c2}(0)$ and (2) the latter evolving steadily toward the temperature-dependent form of the upper critical field $H_{c2}(T)$ observed for conventional superconductors. For $Sm_{2-x}Ce_xCuO_{4-y}$, where superconductivity first appears in the underdoped (UD) region close to $p=1/8$, the $H_g(T)$ lines evolve with Ce doping toward a conventional form of $H_{c2}(T)$ in a manner concordant with those of $Y_{0.8}Ca_{0.2}Ba_2Cu_3O_x$. Furthermore, based upon an analysis

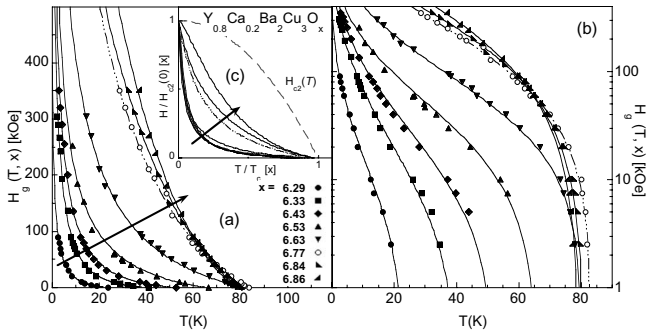

FIG. 1. Vortex melting line H_g vs T data for $Y_{0.8}Ca_{0.2}Ba_2Cu_3O_x$ films. The $H_g(T)$ data was taken in the field range 2.5 kOe$<H<$350 kOe. Fits of the modified vortex glass melting line expression, Eq. (7) of Ref. 14, to the data, are shown in (a) linear and (b) semilog plots to emphasize the quality of the fits over the entire H-T range. Shown in (c) are the extrapolated fit curves to $T=0$ K, $H=H_{c2}(0)$, and the upper critical field $H_{c2}(T)$ for a conventional superconductor, normalized in temperature and field to T_c and $H_{c2}(0)$, respectively.

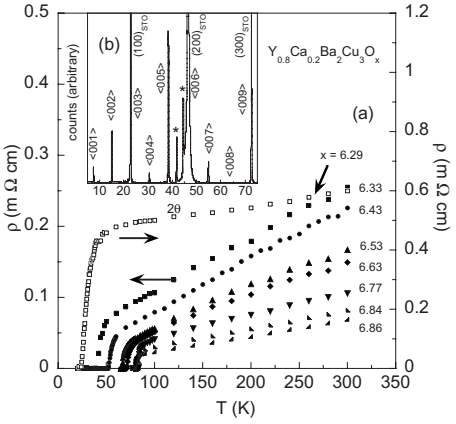

FIG. 2. (a) Electrical resistivity $\rho(T)$ data in zero field for $Y_{0.8}Ca_{0.2}Ba_2Cu_3O_x$ films with the oxygen doping levels indicated. The inset (b) shows x-ray diffraction data for the $x=6.29$ sample. The film is seen to be of high quality with c-axis orientation and no impurities or off-axis peaks are seen. Spurious reflections attributed to the substrate are indicated by asterisks.

of $H_g(T)$, as a function of charge doping p (oxygen/Ce doping x), within the context of a phenomenologically modified model[14,15] of the melting of a vortex solid in high-T_c superconductors,[16] we find evidence that the underlying physics of the 1/8 doping state and the pseudogap are both relevant to the problem of the vortex solid-liquid transition and play an important role in determining the phase boundary $H_g(T)$ in both systems. We point out in advance that some of the results presented below provide further rationalization of conclusions reached in recent important studies which have significantly advanced the understanding of the nature of the pseudogap and its relationship to the superconducting gap, and the likely reconstruction of the Fermi surface. However, in addition to arriving at conclusions, via distinctly different methods of analysis, that are consistent with independent recent work, we develop a perspective of the ground state of high-T_c cuprates, based upon the observed correlation of the strength of quantum-driven vortex fluctuations and the pseudogap energy scale. We suggest that the pseudogap and the superconducting states are independent, and, *that the electronic states belonging to the pseudogap are in a fluctuation regime that is unable to achieve a coherent superconducting state, even at* $T=0$, with the consequence that the electronic states of the pseudogap, which exist at all finite temperatures below the pseudogap temperature T^*, form a population of charge carriers that, in underdoped specimens, appear to behave as "preformed pairs" at temperatures $T>T_c$, but never fully participate in superconductivity as they are unable to achieve phase coherence.

I. EXPERIMENTAL

Films of $Y_{0.8}Ca_{0.2}Ba_2Cu_3O_x$ and $Sm_{2-x}Ce_xCuO_{4-y}$ were used in this study since single crystals grown via the flux method can have nontrivial variations in the dopant concentration (Ca, Ce) within a single batch. In the case of the $Y_{0.8}Ca_{0.2}Ba_2Cu_3O_x$ films, by producing all samples from the same target, we can infer the oxygen content of the samples with greater certainty. In the case of the $Sm_{2-x}Ce_xCuO_{4-y}$ films, the nominal Ce concentration is that of the prepared target material.

Epitaxial $Y_{0.8}Ca_{0.2}Ba_2Cu_3O_x$ films ($6.29 \leq x \leq 6.86$) were grown on (001) $SrTiO_3$ substrates via the pulsed laser ablation method using a 248-nm laser. Following the method of Ref. 18, the target material used for the ablation process was prepared from stoichiometric quantities of Y_2O_3, CaO, $Ba(NO_3)_2$, and CuI. All heating, cooling, and annealing of the target material were carried out under flowing oxygen at a rate of ~ 150 cm^3/min. During the ablation process, the laser beam was focused onto the target over an area of 1 mm$\times$2 mm with an incident energy of 100 mJ. Films were grown at 780 °C in 300 mtorr of flowing oxygen with the incoming gas directed onto the substrate/film. The films were immediately cooled to 450 °C and annealed *in situ* in sealed oxygen atmospheres of 150 mtorr to 900 torr for a period of 4 h. Zero field resistivity and x-ray data (see Fig. 2) confirm the quality of the films and the x-ray data confirms a c-axis orientation. The films were lithographically formed to have dimensions of $\ell \times w \times t \approx 0.3$ cm$\times$0.05 cm $\times$200 nm for electrical transport measurements. The oxygen content of the films was inferred from the T_c vs δ data of Ref. 19 with the error bars representing the uncertainty of x. T_c is determined here by the vanishing of the electrical resisitvity. The hole concentration per copper atom in the CuO_2 planes are estimated via the empirical formula $[T_c(p)/T_{c,max}]=1-82.6(p-0.167)^2$, similar to those used in Refs. 20 and 21 and by comparison to the T_c vs p data of Ref. 22 for $YBa_2Cu_3O_{6+x}$. Having films of thickness $t \approx 200$ nm, we can reasonably rule out strain effects on intrinsic electronic properties.[23,24]

The electron concentration per copper atom, p, in the CuO_2 planes of the $Sm_{2-x}Ce_xCuO_{4-y}$ thin-film samples was estimated here according to the following considerations: in the electron-doped high-T_c cuprate system $R_{2-x}Ce_xCuO_{4+y}$ (R=La, Pr, Nd, Sm, Eu), the substitution of Ce introduces

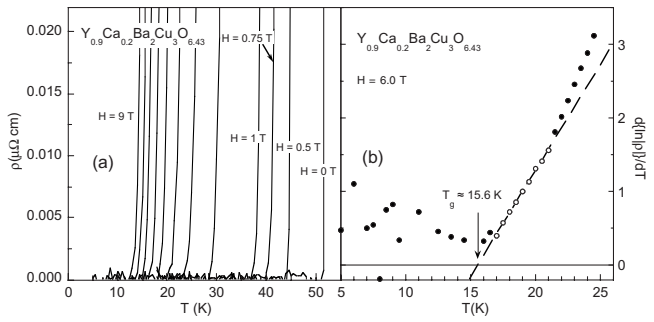

FIG. 3. Low-field resistivity data. (a) Electrical resistivity data $\rho(T)$ of the $Y_{0.8}Ca_{0.2}Ba_2Cu_3O_{6.43}$ film in magnetic fields ranging from 0 to 9 T. Data in fields of 0, 0.5, 0.75, 1.0, and 9 T are indicated. Data taken in fields between 1 and 9 T are in 1 T increments. (b) The vortex-glass melting temperature $T_g \approx 15.6$ K (for $H=6.0$ T) is defined here as the vanishing of the resistivity in the context of the vortex glass model of Fisher, Fisher, and Huse (Ref. 29), where the linear region, when plotted as above, (open circles) defines the critical region of the melting transition. This method of determining T_g was used for all $\rho(T)$ data.

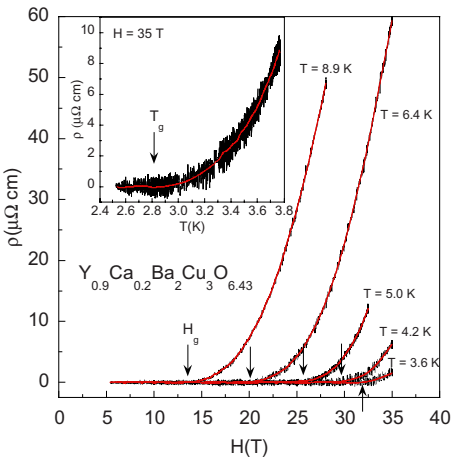

FIG. 4. (Color online) High-field resistivity data. Electrical resistivity data $\rho(H)$ of the $Y_{0.8}Ca_{0.2}Ba_2Cu_3O_{6.43}$ film at fixed temperatures ranging from 3.6 to 8.9 K. The melting field H_g for each temperature is indicated by arrows, where $\rho(H)$ discernibly vanishes. The error associated with each H_g value is no larger than 0.5 T. The $\rho(H)$ data were taken in slow swept fields of 2–3 T/min. Raw data are shown in black. A smoothing algorithm was used to assist in defining H_g. Smoothed data are shown as the red solid line. Shown in the inset are data taken at a fixed field of 35 T. The temperature in this case was controlled by pumping on a He-4 bath which the probe and sample were immersed in.

electrons into the CuO_2 plane. However, a further step is necessary: the reduction in oxygen content by a very small amount. It has recently been established that oxygen doping plays a dual role in these materials: the introduction of itinerant carriers for superconductivity and the reduction in disorder.[25,26] Of the two, it is believed that the disorder effect dominates, and is primarily attributable to oxygen vacancies at the apical (or interstitial) sites and in the CuO_2 plane. With the remaining site located in the CeO layer, where main charge doping process takes place via the rare-earth site, we conclude that this is the most natural location for the introduction of charge via a vacancy at the oxygen site. With an optimal reduction level of oxygen $\delta \sim 0.02$, determined for a $Sm_{1.85}Ce_{0.15}CuO_4$ sample,[27] this gives an approximate oxygen reduction in $\delta/4 \approx 0.005$ of the CeO layer. From this we estimate $p=x+0.005$, for all samples. It should be noted, however, that in the case of nonsuperconducting samples of $Nd_{2-x}Ce_xCuO_{4+y}$, annealed under the same conditions, the oxygen content $4+y$ varies with the Ce concentration level.[28] Hence, the error estimate likely increases for samples with $x \neq 0.15$.

The low field ($H \leq 9$ T) vortex-glass melting line $H_g(T)$ data of the $Y_{0.8}Ca_{0.2}Ba_2Cu_3O_x$ films were determined from the vanishing of $\rho(T)$ data in fixed magnetic fields in the context of the vortex glass model of Fisher, Fisher, and Huse (FFH).[29] See Fig. 3 as an example for the $Y_{0.8}Ca_{0.2}Ba_2Cu_3O_{6.43}$ sample. The high-field ($H>9$ T) $H_g(T)$ data of the $Y_{0.8}Ca_{0.2}Ba_2Cu_3O_x$ films were determined by the vanishing of $\rho(H)$ data at fixed temperatures, as shown in Fig. 4. For the $x=6.43$, 6.77, 6.84, and 6.86 samples, the melting temperature T_g at $H=35$ T was determined by slowly sweeping the temperature, as shown below for the $x=6.43$ sample in the inset of Fig. 4. The melting line $H_g(T)$ data of the $Sm_{2-x}Ce_xCuO_{4-y}$ samples from Ref. 17 were determined using the modified vortex glass model of Rydh, Rapp, and Andersson[30,31] which is based upon the FFH model.

II. ANALYSIS

For the analysis carried out here, four parameters are used to fit Eq. (7) of Ref. 14 to the data; the upper critical field $H_{c2}(0)$, the Lindemann number c_L, an exponent s, and a quantum fluctuation parameter $Q_0 \equiv Q_u(0)\Omega_0\tau_r^p(0)$. The Lindemann number c_L characterizes the stability of the solid vortex ensemble to displacements of vortices from an equilibrium position by quantum and/or thermal fluctuations. The exponent s characterizes the temperature dependence of the relaxation time of a single vortex (SVRT) displaced by a quantum or thermal fluctuation where $\tau_r^p(T) = \tau_r^p(0)[(T_c/T)(1-T/T_c)]^{-s}$. $\tilde{Q}_u(0) = \frac{e^2}{\hbar}\frac{\rho_N}{\epsilon\xi_0}$ is the quantum of resistance, and $\Omega_0 = \min[\Omega_{\mu 0}, \Omega_{\Delta 0}]$ is a cut-off frequency such that, $\Omega_{\mu 0} \propto 1/\sqrt{\rho_N \tau_r^p(0)}$ and $\Omega_{\Delta 0} \propto \Delta_0$.[15] Finally, ρ_N is the normal state resistivity just above T_c, ξ_0 is the $(T=0)$ superconducting coherence length and Δ_0 is the $(T=0)$ superconducting energy gap. The value of the upper critical field is initially estimated from a linear extrapolation (on a semilog scale) of the $H_g(T)$ data to $T=0$, and allowed to vary, along with the other parameters for the best possible fit. The quality of the fit to the data is very sensitive to all four parameters so that we have small errors, less than 5%, associated with each of c_L, s, and Q_0, and less than 2% for $H_{c2}(0)$. Values of c_L, s, Q_0, and $H_{c2}(0)$, for the fits to the data of each of the films examined here, as well as T_c, are given in Appendix B, along with additional details of the fitting procedure.

A. Quantum vortex fluctuations and the pseudogap

In Figs. 5(a) and 5(b), values of the quantum vortex fluctuation parameter $Q_0 \equiv \tilde{Q}_u(0)\Omega_0\tau_r^p(0)$ are plotted vs p (and x)

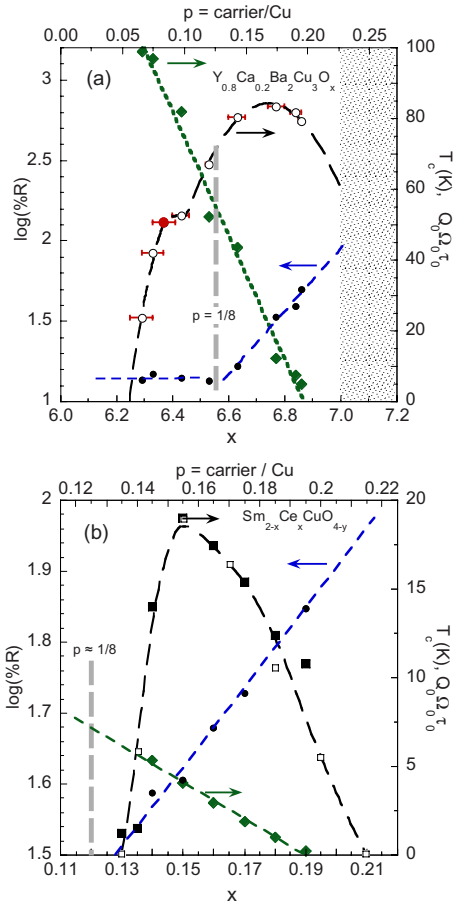

FIG. 5. (Color online) The superconducting critical temperature T_c (a) open circles, (b) open and closed squares), (unitless) quantum vortex fluctuation parameter $Q_0 = \tilde{Q}_u(0)\Omega_0\tau_r^p(0)$ (green solid diamonds), and log(%R) (closed black circles), vs oxygen/Ce content x or carrier/Cu concentration p for: (a) $Y_{0.8}Ca_{0.2}Ba_2Cu_3O_x$ film samples. The x-axis error bars for the T_c vs x (or p) data represent the uncertainty in the oxygen content (carrier/Cu) as described in Sec. I. The $H_g(T)$ line was not measured for the sample indicated by the solid red symbol ($x \approx 6.36$), and hence is not represented in the $Q(0)$ or log(%R) data, or in Fig. 1. (b) $Sm_{2-x}Ce_xCuO_{4-y}$ film samples. T_c vs. x data are taken from Refs. 17 and 36 and are represented by open and closed squares, respectively. The values of p are estimated for both compounds as described in Sec. I.

for $Y_{0.8}Ca_{0.2}Ba_2Cu_3O_x$ and $Sm_{2-x}Ce_xCuO_{4-y}$, respectively. In both cases, Q_0 is seen to have a linear dependence with p and x across the entire range of doping examined with $Q_0 \to 0$ at a critical concentration $p_c \approx 0.195$. This behavior immediately brings to mind the linear T-x behavior of the pseudogap temperature $T^*(x)$, which extrapolates linearly to $T=0$ in the vicinity of $p \approx 0.19-0.20$.[8,10,32] Since the dynamical properties of vortices are directly dependent upon the nature of the electronic states within the vortex core,[33] then, with evidence from scanning tunneling microscope measurements of pseudogap states within the vortex core,[34] it seems natural to associate the strength of quantum vortex fluctuations, characterized by Q_0, with the strength of the pseudogap. If such a connection is valid, then one can ask—what does $Q_0 \to 0$ mean?

As $T \to 0$, the quantum of resistance remains finite. For the cut-off frequency Ω, we have either $\Omega_{\mu 0} \propto 1/\sqrt{\rho_N \tau_r^p(0)}$ or $\Omega_{\Delta 0} \propto \Delta_0$,[15] from which it follows $\Omega_{\mu 0}\tau_r^p(0) \propto \sqrt{\frac{\tau_r^p(0)}{\rho_N}}$ or $\Omega_{\Delta 0}\tau_r^p(0) \propto \Delta_0 \tau_r^p(0)$. Thus, for Q_0 to vanish, either case implies that $\tau_r^p(0) \to 0$; i.e., quantum fluctuations of vortices cease, with only thermally driven vortex fluctuations remaining. In the above model, the empirically deduced temperature dependence of the SVRT, τ_r^p, can be explained by the quasiparticles within the vortex core conforming to a relaxation time consistent with fluctuating Cooper pairs in a critical regime, i.e., the dominant population of quasiparticles in the vortex core are in a fluctuation regime rather than being Drude-type.[14,15,35] In this context, the result $\tau_r^p(0) \to 0$ indicates that the quasiparitcle population in the fluctuation regime vanishes as $p \to p_{c2} \approx 0.195$, and, that, as the system moves to larger values of p, the vortex cores will be primarily populated by conventional Drude-type quasipartices. This viewpoint is consistent with the results of Cooper *et al.*[13] wherein their observation of a significant change in the dominant normal state quasiparticle properties from coherent to incoherent transport can be identified here with the transition from a Drude-type to a fluctuationlike form of the SVRT τ_r^p with decreasing doping at p_c. It follows that a connection can be made between the quasiparticles in the pseudogap state and strong quantum driven fluctuations of vortices. Furthermore, from heat capacity measurements on $Y_{0.8}Ca_{0.2}Ba_2Cu_3O_{7-\delta}$,[32] it is found that, while the energy scale E_g associated with the pseudogap approaches zero linearly as $p \to 0.19$, E_g in fact remains finite, tailing off to at least $p \approx 0.22$, a value close to the oxygen doping limit in this compound. Thus, if the correlation between Q_0 and E_g holds, we would then expect Q_0 (for $Y_{0.8}Ca_{0.2}Ba_2Cu_3O_x$ at least), to also remain finite for $p > p_{c2}$ in a manner proportional to the values E_g and consistent with the residual α_1 (T-linear) resistivity component associated with the pseudogap.[13]

B. "Conventionality" parameter R

With growing evidence for a two-fluid conductivity scenario and the relative increase of the Fermi-liquidlike (T^2 resistivity) component as p increases, we might anticipate that superconducting properties will evolve with increased doping toward that found in conventional superconductors. In this vein, we attempt to characterize the "extent of conventionality" across the $Y_{0.8}Ca_{0.2}Ba_2Cu_3O_x$ and $Sm_{2-x}Ce_xCuO_{4-y}$ systems by considering how closely their $H_g(T)$ lines resemble the canonical form of the upper critical field of a conventional BCS superconductor, which can be approximated as $H_{c2}(T) \approx H_{c2}(0)[1-(T/T_c)^2]$. We introduce a measure of conventionality via the number R, defined as the ratio of the area in the H-T plane under the fitted $H_g(T)$ curve to the area under the BCS upper critical field with the same $H_{c2}(0)$ and T_c values, $R \equiv [\int_0^{T_c} H_g(T)dT]/[\int_0^{T_c} H_{c2}(T)dT]$.

In Figs. 5(a) and 5(b), we have plotted log(%R) $\equiv$ log(100 × R) vs p (and x), where %R is the "percentage of conventionality," and a value of log(%R)=2 corresponds to "complete conventionality." Two key features are observed.

First, in the case of $Y_{0.8}Ca_{0.2}Ba_2Cu_3O_x$, for doping values $p < p_{c1} \approx 1/8$, $\log(\%R)$ is independent of p. However, for $p \gtrsim p_{c1}$, the p dependence of $\log(\%R)$ abruptly increases linearly, where, (the second important observation) $\log(\%R)$ in this region extrapolates to a value of 2, i.e., "conventional superconductivity," just as the limits of oxygen doping are reached at $x=7.0$ ($p \approx 0.225$). This scenario is consistent with the results of Cooper *et al.*,[13] wherein the non-Fermi-liquidlike T-linear contribution to the resistivity extends out past the superconducting dome and hence pure Fermi-liquid behavior is not recovered before superconductivity expires. In the case of $Sm_{2-x}Ce_xCuO_{4-y}$, (where superconductivity appears for $p \gtrsim 1/8$), the same linear with p dependence of $\log(\%R)$ is also observed over the same range of p, and $\log(\%R)$ also extrapolates to a value of 2 at $p \approx 0.225$. This conclusion should be taken with some caution, since, in both cases, we lack data on samples with concentrations $p > p_{c2} \approx 0.195$ where p_{c2} is the putative QCP associated with the suggested termination of the pseudogap at $T=0$. If p_{c2} is in fact a QCP, then we could anticipate a change in the p dependence of $\log(\%R)$ as we cross over from one ground state to another. Additionally, had we chosen a different form for $H_{c2}(T)$, the value of R would change accordingly, and hence the conclusion as to whether or not conventional superconductivity is reached by $p \approx 0.225$ is subject to further reservation. For instance, it is possible that the apparent existence of two superconducting bands could result in a modification of $H_{c2}(T)$ such that,[37] if the observed linear dependence of $\log(\%R)$ on p persists, then $H_g(T)$ and $H_{c2}(T)$ would coincide at a lower oxygen concentration. We however stress that, even with a different expression for $H_{c2}(T)$, the abrupt change in $\log(\%R)$ at $p \lesssim 1/8$ for $Y_{0.8}Ca_{0.2}Ba_2Cu_3O_x$ would remain, as can be easily seen from the simply scaled $H_g(T)$ data in Fig. 1(c), as would the conclusion that the electronic states above and below $p_{c1} \approx 1/8$ are significantly different—a result consistent with a reconstruction of the Fermi surface.[1]

III. CONCLUSIONS

The independent behavior (with doping) of the quantum vortex fluctuation parameter $Q(0)$ and the conventionality parameter $\log(\%R)$ of $Y_{0.8}Ca_{0.2}Ba_2Cu_3O_x$ suggests that phenomena associated with the pseudogap, on the one hand, and the 1/8 doping state, on the other, are independent as well, and hence there exist coexisting electronic populations, both of which have an impact on the evolution of superconducting properties across the $T_c(p)$ dome.

An implication of a connection between the size of the pseudogap and the magnitude of the quantum parameter Q_0 is that for $p \leq p_{c2} \approx 0.195$, a significant portion of the electronic states in the "normal" vortex core belong to the pseudogap, and, most importantly, that these electrons are in a fluctuation regime. In addition to the empirically observed form of the SVRT, the notion that the pseudogap states are in an incoherent precursor state to that of coherent bulk superconductivity is supported by evidence for the presence of vortices in the pseudogap phase above T_c from Nernst effect[38] and magnetoresistance[39] measurements, and by a quantitative analysis of zero field fluctuation conductivity.[40] From the form of the empirically observed single vortex relaxation time τ_r^v and its direct relationship to the value of Q_0 with doping, we also conclude that *the pseudogap states remain in a fluctuation regime down to* $T=0$. We are then left with a picture similar to the low lying "extended quantum phase" proposed by Cooper *et al.*,[13] expanded to include both hole- and electron-doped high-T_c cuprates, wherein we would conclude that the electrons comprising the pseudogap are electronic states that are unable to achieve a coherent superconducting phase at any finite temperature, and, that these electrons are distinct from those which form the superfluid condensate. We emphazise that our proposition as to the (quantum-driven) fluctuating nature of the pseudogap state is unique, even though the conclusion of the independence of the pseudogap and superconducting states has been arrived at in earlier work.[41] Within the scenario we are proposing, we can explain the long-standing contradiction between experiments which support the pseudogap as preceding the superconducting state and those that indicate that they are competing states. That is, the experiments and analyses in Refs. 38–40 (and similar papers) can be explained in terms of the fluctuating nature of the pseudogap without having to contradict other experiments that indicate that the pseudogap state is not a precursor to the superconducting state.

Finally, we would suggest at least two issues to be addressed within the realm of high-T_c superconductivity: (1) a theoretical explanation is lacking to explain the abrupt change in the temperature dependence of $H_g(T)$ of the $Y_{0.8}Ca_{0.2}Ba_2Cu_3O_x$ system at $p=1/8$, and the linear p dependence of $\log(\%R)$ of both the $Y_{0.8}Ca_{0.2}Ba_2Cu_3O_x$ and $Sm_{2-x}Ce_xCuO_{4-y}$ systems in the $p > 1/8$ region and (2) an implication of the assertion that the pseudogap is in a fluctuating superconducting state, independent of the true phase coherent superconducting state, is that the fluctuations of the pseudogap charge carriers will affect measurements of critical scaling phenomena. Specifically, it is a long-standing question as to why the scaling behavior of certain (superconducting state) phenomena of the cuprates do not conform to a pure three-dimensional- (3D-) XY model. A theoretical treatment of coexisting fluctuation phenomena belonging to different universal classes may provide such an explanation.

ACKNOWLEDGMENTS

This research was sponsored by the U.S. Department of Energy (DOE) under Research Grant No. DE-FG02-04ER46105. A portion of this work was performed at the National High Magnetic Field Laboratory, which is supported by NSF Cooperative Agreement No. DMR-0084173, by the State of Florida, and by the DOE.

APPENDIX A: SUMMARY 3D PLOT OF *H-T-p* PHASE DIAGRAM

Depicted in Fig. 6 is a 3D summary plot of the resulting *H-T-p* phase diagram of hole-doped cuprates. At temperatures/fields below the colored vortex-glass $H_g(T,p)$ surface, the system is in the superconducting solid vortex

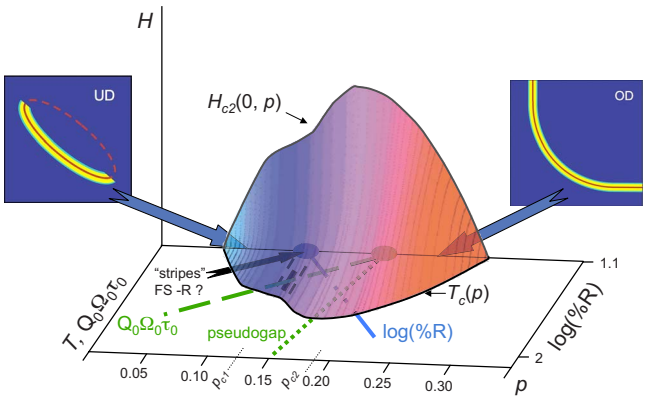

FIG. 6. (Color online) A summary sketch of the *H*-*T*-*p* phase diagram of hole-doped cuprate-based high-T_c superconductors, based upon the analysis and references given in the text. At temperatures/fields below the colored vortex-glass $H_g(T,p)$ surface, the system is in the superconducting solid vortex state. The panels labeled UD and OD are cartoon depictions of the Fermi surface of the highly underdoped and highly overdoped regions, respectively, as inferred by results from quantum oscillation experiments (Refs. 1 and 42–46). The blue and purple shaded regions are directly based upon the $H_g(T,p)$ data of the $Y_{0.8}Ca_{0.2}Ba_2Cu_3O_x$ system examined in this study. The red-shaded region is calculated based upon the observed evolution of $H_g(T)$ with carrier/Cu concentration p. It is proposed that the strength of quantum-driven vortex fluctuations is directly attributable to the transport properties of electrons belonging to the pseudogap. If this connection is valid then we can conclude that the electronic states belonging to the pseudogap are in a fluctuation regime that is unable to achieve a fully superconducting state, even at $T=0$. Hence, the pseudogap and bulk superconductivity are distinct phenomena in the high-T_c cuprates.

state. As shown, the $H_g(T,p)$ phase diagram is broken up into three roughly equal (in range of hole doping p) regions having distinct electronic characteristics. The left (highly underdoped) blue region is characterized by having a disconnected Fermi surface (as indicated in the "UD" Fermi surface cartoon) and a superconducting state subjected to increasingly strong destabilizing quantum-driven vortex fluctuations (with decreasing p). In the center (lightly underdoped to lightly overdoped) purple region, the Fermi surface has undergone a reconstruction at its underdoped border p_{c1} evolving toward that of a conventional metal. The strength of quantum-driven vortex fluctuations approaches zero with a linear in p dependence at the overdoped border p_{c2} with the red (highly overdoped) region on the right *as does the pseudogap line*. In the red region beyond p_{c2}, the Fermi surface has completed its transformation [overdoped (OD) Fermi surface cartoon] and the $H_g(T,p)$ lines continue to evolve toward the upper critical field lines $H_{c2}(T)$ as the decreasingly residual pseudogap population vanishes along with quantum-driven vortex fluctuations. As T_c decreases with increasing p, the importance of thermal fluctuations will also decrease and eventually $H_g(T)$ will coincide with $H_{c2}(T)$. From the perspective of the performance of high-T_c cuprates in high-field applications, the optimal carrier concentration is p_{c2}. At this concentration, T_c is approximately 90% of the maximum T_c value found near the center of the purple region, yet, the value of $H_g(T,p_{c2})$ is greater than $H_g(T,p_{opt})$ for over more than 90% of its temperature range, with the consequence that higher critical current densities can be achieved over this temperature interval. As an example, for the $Y_{0.8}Ca_{0.2}Ba_2Cu_3O_x$ system, at liquid helium temperatures, $H_g(4.2\ \mathrm{K},p_{c2})\approx 1.5H_g(4.2\ \mathrm{K},p_{opt})$. At liquid nitrogen temperatures, $H_g(77\ \mathrm{K},p_{c2})\approx H_g(77\ \mathrm{K},p_{opt})$.

TABLE I. Doping dependence of the fitting parameters c_L, s, $Q_0\Omega_0\tau_0$, and $H_{c2}(0)$ used in the fitting of Eq. (7) of Ref. 14 to the $H_g(T)$ data shown in Fig. 1. The errors of the parameters for all fits is $\Delta c_L\approx 0.015$, $\Delta s\approx 0.10$, $\Delta Q\approx 5\%$, and $H_{c2}(0)\approx 2\%$. Also given are values of T_c, defined here as the temperature at which the resistivity vanishes.

x	c_L	s	$Q_0\Omega_0\tau_0$	$H_{c2}(0)$ (T)	T_c (K)
6.86	0.30	2.70	4.9	135.0	79.1
6.84	0.30	1.95	7.4	138.5	81.7
6.77	0.29	2.10	12.2	149.2	83.5
6.63	0.29	1.94	39.3	146.5	80.4
6.53	0.31	2.00	52.0	120.8	67.0
6.43	0.29	2.36	82	87.0	52.5
6.33	0.31	2.53	97	69.0	41.9
6.29	0.30	2.36	99	39.1	23.6

APPENDIX B: FITTING METHODS AND TABLES OF PARAMETERS

The procedure for fitting the subsequent $H_g(T)$ data of each sample is described in detail in Ref. 14, with the only difference being that, for the data fit here, the value of $H_{c2}(0)$ was estimated, as described in the main text, and allowed to vary to achieve the best possible fit. In Ref. 14, values of $H_{c2}(0)$ were taken from the literature and held fixed during the fitting process. For clarity, we reemphasize here, the steps for fitting the data are: (1) an initial estimate of $H_{c2}(0)$ is obtained from a linear extrapolation (on a semilog plot) to

TABLE II. Doping dependence of the fitting parameters c_L, s, $Q_0\Omega_0\tau_0$, and $H_{c2}(0)$ used in the fitting of Eq. (7) of Ref. 14 to the $H_g(T)$ data taken from Ref. 17. The errors of the parameters for all fits is $\Delta c_L\approx 0.015$, $\Delta s\approx 0.10$, $\Delta Q\approx 5\%$, and $H_{c2}(0)\approx 2\%$. Also given are values of T_c, defined here as the temperature at which the resistivity vanishes.

x	c_L	s	$Q_0\Omega_0\tau_0$	$H_{c2}(0)$ (T)	T_c (K)
0.13					1.2
0.135					1.5
0.14	0.228	2.03	5.34	6.13	14.0
0.15	0.233	1.86	4.06	8.43	19.0
0.16	0.230	2.23	2.94	4.5	17.43
0.17	0.230	1.80	1.86	4.1	15.4
0.18	0.236	1.97	0.98	2.3	12.38
0.19	0.233	3.72	0.21	2.1	10.8

$T=0$ K of the experimentally determined $H_g(T)$ data. (2) An expression for $G_i(T)$ is obtained by first evaluating $G_i(H_g) = [G_i(0)]^{1/2\alpha}[H_g/H_{c2}(0)]^{1/\alpha}$, where α is the exponent that characterizes the $H_g(T)$ line over the temperature range $0.6\ T_c \leq T \leq T_c$ via the expression $H_g(T) \sim (1-T/T_c)^{\alpha}$. The value of $G_i(0)$ is related to the fitting parameter c_L (the Lindemann number) by the expression $G_i(0)=(\pi^2 c_L^4)^{2\alpha}$. c_L is initially estimated as 0.30, as this is a commonly found value for the high-T_c cuprates.[33] $G_i(T)$ is obtained by fitting a third-order polynomial to the calculated $G_i(H_g)$ data. This expression for $G_i(T)$ is inserted into Eq. (7) of Ref. 14. (3) The data are fit using Eq. (7) keeping $H_{c2}(0)$ fixed, with the remaining fitting parameters s, c_L, and $Q \equiv Q_0\Omega_0\tau_0$ allowed to vary (Tables I and II). (4) Keeping s, c_L, and Q fixed, the data are refit allowing $H_{c2}(0)$ to vary. (5) The new value of $H_{c2}(0)$ is used, and the procedure is repeated at step (2) until there is less than ≈5% variation in the values of s, c_L, Q, and ≈2% in $H_{c2}(0)$. (If the new value of $H_{c2}(0)$ does not result in an improved fit after two iterations, a new trial value of $H_{c2}(0)$ is introduced, and the process repeated). The data were fit using the commercially available software program KALEIDAGRAPH v. 3.51.

[1] N. Doiron-Leyraud, C. Proust, D. LeBoeuf, J. Levallios, J.-B. Bonnemaison, R. Liang, D. A. Bonn, W. N. Hardy, and L. Taillefer, Nature (London) **447**, 565 (2007).

[2] T. Timusk and B. Statt, Rep. Prog. Phys. **62**, 61 (1999).

[3] M. R. Norman, D. Pines, and C. Kallin, Adv. Phys. **54**, 715 (2005).

[4] V. J. Emery, S. A. Kivelson, and J. M. Tranquada, Proc. Natl. Acad. Sci. U.S.A. **96**, 8814 (1999).

[5] E. Berg, E. Fradkin, and S. A. Kivelson, Phys. Rev. B **79**, 064515 (2009).

[6] V. M. Krasnov, A. Yurgens, D. Winkler, P. Delsing, and T. Claeson, Phys. Rev. Lett. **84**, 5860 (2000).

[7] J. E. Sonier, J. H. Brewer, R. F. Kiefl, R. I. Miller, G. D. Morris, C. E. Stronach, J. S. Gardner, S. R. Dunsiger, D. A. Bonn, W. N. Hardy, R. Liang, and R. H. Heffner, Science **292**, 1692 (2001).

[8] Jing Xia, E. Schemm, G. Deutscher, S. A. Kivelson, D. A. Bonn, W. N. Hardy, R. Liang, W. Siemons, G. Koster, M. M. Fejer, and A. Kapitulnik, Phys. Rev. Lett. **100**, 127002 (2008).

[9] *Handbook of High-Temperature Superconductivity*, edited by J. R. Schrieffer and J. S. Brooks (Springer, New York, 2007).

[10] T. Kawakami, T. Shibauchi, Y. Terao, and M. Suzuki, Phys. Rev. B **74**, 144520 (2006).

[11] S. A. Kivelson, I. P. Bindloss, E. Fradkin, V. Oganesyan, J. M. Tranquada, A. Kapitulnik and C. Howald, Rev. Mod. Phys. **75**, 1201 (2003).

[12] J. E. Sonier, S. A. Sabok-Sayr, F. D. Callaghan, C. V. Kaiser, V. Pacradouni, J. H. Brewer, S. L. Stubbs, W. N. Hardy, D. A. Bonn, R. Liang, and W. A. Atkinson, Phys. Rev. B **76**, 134518 (2007).

[13] R. A. Cooper, Y. Wang, B. Vignolle, O. J. Lipscombe, S. M. Hayden, Y. Tanabe, T. Adachi, Y. Koike, M. Nohara, H. Takagi, C. Proust, and N. E. Hussey, Science **323**, 603 (2009).

[14] B. J. Taylor and M. B. Maple, Phys. Rev. B **76**, 014517 (2007).

[15] B. J. Taylor, D. J. Scanderbeg, M. B. Maple, C. Kwon, and Q. X. Jia, Phys. Rev. B **76**, 014518 (2007).

[16] G. Blatter and B. Ivlev, Phys. Rev. Lett. **70**, 2621 (1993).

[17] D. J. Scanderbeg, Ph.D. thesis, University of California, 2007; D. J. Scanderbeg, B. J. Taylor, R. E. Baumbach, and M. B. Maple (to be published).

[18] X. G. Zheng, M. Suzuki, C. Xu, H. Kuriyaki, and K. Hirakawa, Physica C **271**, 272 (1996).

[19] B. Fisher, J. Genossar, C. G. Kuper, L. Patlagan, G. M. Reisner, and A. Knizhnik, Phys. Rev. B **47**, 6054 (1993).

[20] S. H. Naqib, J. R. Cooper, J. L. Tallon, and C. Panagopoulos, Physica C **387**, 365 (2003).

[21] M. -P. Delamare, K. R. Schöppl, J. D. Pedarnig, and D. Bäuerle, Physica C **372-376**, 638 (2002).

[22] R. Liang, D. A. Bonn, and W. N. Hardy, Phys. Rev. B **73**, 180505(R) (2006).

[23] H. Y. Zhai and W. K. Chu, Appl. Phys. Lett. **76**, 3469 (2000).

[24] J. D. Pedarnig, R. Rössler, M. P. Delamare, W. Lang, D. Bäuerle, A. Kšhler and H. W. Zandbergen, Appl. Phys. Lett. **81**, 2587 (2002).

[25] J. S. Higgins, Y. Dagan, M. C. Barr, B. D. Weaver, and R. L. Greene, Phys. Rev. B **73**, 104510 (2006).

[26] H. J. Kang, P. Dai, B. J. Campbell, P. J. Chupas, S. Rosenkranz, P. L. Lee, Q. Huang, S. Li, S. Komiya, and Y. Ando, Nature Mater. **6**, 224 (2007).

[27] B. C. Chang, Y. Y. Hsu, and H. C. Ku, Physica B **312-313**, 59 (2002).

[28] Y. Tanaka, T. Motohashi, M. Karppinen, and H. Yamauchi, J. Solid State Chem. **181**, 365 (2008).

[29] D. S. Fisher, M. P. A. Fisher, and D. A. Huse, Phys. Rev. B **43**, 130 (1991).

[30] A. Rydh, Ö. Rapp, and M. Andersson, Phys. Rev. Lett. **83**, 1850 (1999).

[31] M. Andersson, A. Rydh, and Ö. Rapp, Phys. Rev. B **63**, 184511 (2001).

[32] G. V. M. Williams, J. L. Tallon, and J. W. Loram, Phys. Rev. B **58**, 15053 (1998).

[33] B. J. Taylor and M. B. Maple, Phys. Rev. B **76**, 184512 (2007).

[34] Ch. Renner, B. Revaz, K. Kadowaki, I. Maggio-Aprile, and O. Fischer, Phys. Rev. Lett. **80**, 3606 (1998).

[35] B. J. Taylor and M. B. Maple, in *Superconducting Cuprates: Properties, Preparation and Applications*, edited by K. N. Courtlandt (Nova Science, Hauppauge, NY, 2009).

[36] Y. Krockenberger, J. Kurian, A. Winkler, A. Tsukada, M. Naito, and L. Alff, Phys. Rev. B **77**, 060505(R) (2008).

[37] M. Mansor and J. P. Carbotte, Phys. Rev. B **72**, 024538 (2005).

[38] Y. Wang, N. P. Ong, Z. A. Xu, T. Kakeshita, S. Uchida, D. A. Bonn, R. Liang, and W. N. Hardy, Phys. Rev. Lett. **88**, 257003 (2002).

[39] V. Sandu, E. Cimpoiasu, T. Katuwal, C. C. Almasan, Shi Li, and M. B. Maple, Phys. Rev. Lett. **93**, 177005 (2004).

[40] B. Leridon, A. Défossez, J. Dumont, J. Lesueur, and J. P. Contour, Phys. Rev. Lett. **87**, 197007 (2001).

[41] J. L. Tallon and J. W. Loram, Physica C **349**, 53 (2001).

[42] N. E. Hussey, M. Abdel-Jawad, A. Carrington, A. P. Mackenzie,

and L. Balicas, Nature (London) **425**, 814 (2003).
[43] B. Vignolle, A. Carrington, R. A. Cooper, M. M. J. French, A. P. Mackenzie, C. Jaudet, D. Vignolles, C. Proust, and N. E. Hussey, Nature (London) **455**, 952 (2008).
[44] D. LeBoeuf, N. Doiron-Leyraud, J. Levallois, R. Daou, J.-B. Bonnemaison, N. E. Hussey, L. Balicas, B. J. Ramshaw, R. Liang, D. A. Bonn, W. N. Hardy, S. Adachi, C. Proust, and L. Taillefer, Nature (London) **450**, 533 (2007).
[45] C. Jaudet, D. Vignolles, A. Audouard, J. Levallois, D. LeBoeuf, N. Doiron-Leyraud, B. Vignolle, M. Nardone, A. Zitouni, R. Liang, D. A. Bonn, W. N. Hardy, L. Taillefer, and C. Proust, Phys. Rev. Lett. **100**, 187005 (2008).
[46] S. E. Sebastian, N. Harrison, E. Palm, T. P. Murphy, C. H. Mielke, R. Liang, D. A. Bonn, W. N. Hardy, and G. G. Lonzarich, Nature (London) **454**, 200 (2008).